

Metal oxide-based gas sensors for the detection of exhaled breath markers

Fereshteh Vajhadin¹ | Mohammad Mazloun-Ardakani¹ | Abbas Amini²

¹Department of Chemistry, Faculty of Science, Yazd University, Yazd, Iran

²Department of Mechanical Engineering, Australian College of Kuwait, Safat, Kuwait

Correspondence

Mohammad Mazloun-Ardakani,
Department of Chemistry, Faculty of Science, Yazd University, Yazd 89195-741, Iran.

Email: mazloun@yazd.ac.ir

Funding information

Yazd University

Abstract

Exhaled breath test is a typical disease monitoring method for replacing blood and urine samples that may create discomfort for patients. To monitor exhaled breath markers, gas biomedical sensors have undergone rapid progress for non-invasive and point-of-care diagnostic devices. Among gas sensors, metal oxide-based biomedical gas sensors have received remarkable attention owing to their unique properties, such as high sensitivity, simple fabrication, miniaturization, portability and real-time monitoring. Herein, we reviewed the recent advances in chemoresistive metal oxide-based gas sensors with ZnO, SnO₂ and In₂O₃ as sensing materials for monitoring a range of exhaled breath markers (i.e., NO, H₂, H₂S, acetone, isoprene and formaldehyde). We focused on the strategies that improve the sensitivity and selectivity of metal oxide-based gas sensors. The challenges to fabricate a functional gas sensor with high sensing performance along with suggestions are outlined.

KEYWORDS

exhaled breath marker, gas medical sensor, metal oxide, nanomaterial, non-invasive disease diagnosis, point-of-care device, selective detection

1 | INTRODUCTION

Breath analysis is a promising approach for monitoring diseases and their progression as it provides a non-invasive, very safe and simple way for all patients as many times as needed. The exhaled breath markers (EBMs) compose of inorganic compounds (e.g. carbon dioxide, carbon monoxide and nitric oxide), voltaic organic compounds (e.g. isoprene, formaldehyde, and acetone) and non-voltaic compounds (e.g. cytokines and hydrogen peroxide; Cazzola & Novelli, 2010; Kim, Jahan, et al., 2012; Lu et al., 2018; Wang & Sahay, 2009). The abnormal level of EBM carries some information about the disease status and treatment efficiency (Das & Pal, 2020). Many clinical trials focused on EBM for the diagnosis of disease ranging from respiratory, diabetes to cancer (Brinkman et al., 2020; Chang et al., 2018; Gregis et al., 2018; Kabir et al., 2019; Rahman et al., 2020).

To monitor EBM, various techniques have been utilized, such as chromatography, selected ion flow tube-mass spectrometry (SIFT-MS), proton-transfer reaction-mass spectrometry (PTR-MS) and

laser spectroscopy technique (Das & Pal, 2020; Kharitonov & Barnes, 2002; Kim, Jahan, et al., 2012). Among them, chromatography-mass spectrometry (GC-Mass) is a well-established method in clinical trials for monitoring EBM, owing to its outstanding precision and selectivity (Wang & Sahay, 2009). However, GC-Mass application often is limited to laboratory usage due to requiring sophisticated, bulky and high-cost instruments, and experts (Glockler et al., 2020). To date, the advances in portable gas sensors with the miniaturized size hold great potential to overcome such shortcomings and pave the way for point-of-care EBM monitoring.

Chemoresistive metal oxide-based gas sensors (MGSs) identify the target gas by using a change in electrical resistance that translates to the gas concentration. Recently, MGS has received much attention given for their great potential in breath analysis owing to the advantages such as straightforward integration in a chip, simple manufacturing, high stability and reusability (Cho et al., 2017; Das & Pal, 2020; Guntner et al., 2019; Tai et al., 2020). The metal oxides are categorized into n-type and p-type. In the n-type MGS, adsorbed

air oxygen onto the metal oxide receives electrons from metal oxide via conduction bands. This electron transformation causes a reduction in carrier charges in metal oxide surface and formation of the depletion layer and also the formation of oxygen ions (O^{2-} , O^- or O^{2-}) (Moseley, 2017). The reducing target gas takes electrons from oxygen ions and transport electrons to the conduction band of metal oxides resulting in an increasing conductivity and reducing resistance. In the case of exposure to the oxidizing target gas, the overall result reduces the conductivity. In the p-type metal oxide, the adsorbed oxygen traps the electron through the valance band of metal oxide that results in generation holes. The effect of exposure to the reducing or oxidizing target gases on the conductivity is the reverse of n-type cases. Beyond n-type or p-type metal oxide as a sensing material, combining metal oxides with other metal oxides, noble metals and carbon-based materials might generate p-p, n-p and n-n type heterojunctions and potentially further enhance the electron mobility (Amiri et al., 2020).

Herein, we focus on MGS for disease diagnosis by EBM. Subsequent sections indicate the current state of gas sensors based on the three most common metal oxides including ZnO, SnO₂ and In₂O₃ with paying attention to the role of nanomaterials in enhancing the analytical performance of the sensors. We also describe recent progress in gas sensors along with the strategies to improve their sensing performance.

2 | EXHALE BREATH MARKERS

Exhaled breath composes of more than a thousand gases of which some of these gases are known as EBM that any variations in their concentrations initiate disorders and diseases. The most common EBM and their corresponding disease are briefed in Table 1. As shown in some cases, the abnormality in EBM renders several diseases, while several EBMs might be attributed to particular diseases. Still, the exploration of breath analysis in the clinics is very immature. There are great challenges for the standardization of EBM assessments that include but not limited to inter-individual variability stemming from genetics, human activities or air pollutions. Despite

such challenges, there is remarkable progress in revealing the connection between EBM and disorders (Guntner et al., 2019). The identification of acetone as EBM for diagnosis of diabetic people backs to 1857 (Crofford et al., 1977) resuming with continuous efforts on the investigation of EBM to accurately diagnose diseases.

In a recent study, by taking benefits from data analysis methods, seven biomarkers for the discrimination of lung cancer patients from healthy ones were named as acetone, methyl acetate, isoprene, methyl vinyl ketone, cyclohexane, 2-methylheptane and cyclohexanone (Rudnicka et al., 2019). To date, by utilizing nanomaterials into sensors, the exhaled breath analysis has become more achievable for rapid and painless disease diagnostic.

3 | METAL OXIDE-BASED GAS SENSORS FOR THE DETECTION OF EXHALED BREATH MARKERS

The analytical performance of gas sensors at the operating temperature and relative humidity (RH) is determined with the following characteristics. (i) *Selectivity*: the main challenge in MGS is selectivity for the accurate detection of EBM that often is modulated by the type and amount of dopants, grain size, morphologies and preparation protocols (Kim, Kim, et al., 2012; Kim, Choi, et al., 2016). The selectivity of metal oxide-based gas sensors is often reduced in the interferences of water vapours (Liu et al., 2020). It is of note that the RH of human breath is about 89%–97% (Ferrus et al., 1980). (ii) *Limit of detection (LOD)*: the EBM concentration is in the range of ppb-ppt, and the MGS should have high sensitivity for detection of trace level of EBM (Das & Pal, 2020). (iii) *Stability*: MGS should be stable to generate reliable and reproducible results. In the following, we will discuss recent MGS with the focus on ZnO, SnO₂ and In₂O₃. These metal oxides are n-type semiconductors, meaning that they have a similar mechanism in response to the oxidizing/reducing target gas (Zhang, Liu, et al., 2016). Due to taking benefit from the high electron mobility, they use as sensitive platforms for the detection of gases (Ho et al., 2011; Zhang, Zhou, et al., 2016). Among these three metal oxides, ZnO has been extensively studied

TABLE 1 Exhale breath markers and corresponding diseases

Biomarker	Disease	Reference
Acetone (OC(CH ₃) ₂)	Diabetes, lung cancer, congestive heart failure	Hanh et al. (2020), Ruzsanyi and Peter Kalapos (2017), Wang and Sahay (2009)
Isoprene	Blood cholesterol level, lipid disorder, fibrosis and cirrhosis	Alkhouri et al. (2015), Salerno-Kennedy and Cashman (2005)
Nitrogen monoxide (NO)	Asthma, chronic obstructive pulmonary disease (COPD), lung disease, airway inflammation, hypertension, rhinitis, cystic fibrosis	Barnes et al. (2006), Birrell et al. (2006), Brindicci et al. (2005), Cazzola and Novelli (2010), Guntner et al. (2019), Kharitonov and Barnes (1996, 2002), Lu et al. (2018), McCluskie et al. (2004), Wang and Sahay (2009)
Formaldehyde (HCHO)	Lung cancer	Wehinger et al. (2007)
Hydrogen (H ₂)	Intestinal upset, indigestion in infants	Wang and Sahay (2009)
Hydrogen sulphide (H ₂ S)	Asthma, chronic obstructive pulmonary disease (COPD)	Bulemo et al. (2017), Chung (2014), Zhang et al. (2015)

in medical gas sensors due to low toxicity, ease of preparation and cost-effectiveness (Wei et al., 2011). Compared to ZnO, SnO₂ and In₂O₃ standing out for their high stability (Bulemo et al., 2017) The operational temperature of these metal oxides often is high (150–400°C) (Zhang, Liu, et al., 2016). Integration of these metal oxides with noble metal elements and carbon nanostructures is importance as it might lower their operational temperature to room temperature. Table 2 summarizes recent MGS with their key characteristics for EBM detection.

3.1 | ZnO-based gas sensors

ZnO is a very active semiconductor metal oxide for disease monitoring due to its excellent biocompatibility, low cost and environmental friendliness. ZnO morphology adjustment is important to maximize the interaction between the adsorbed oxygen and the target gas and thereby the sensitivity of MGS. Sensitivity and selectivity of ZnO-based metal oxides are often tailored via integration with other metal oxides (e.g. CuO) and noble metal elements that might tune the Schottky barrier modulation and provide multiple p-n heterojunctions (Kim, Jahan, et al., 2012; Li et al., 2019).

In recent years, the modification of ZnO with CuO for MGS has received remarkable attentions. Various morphologies of ZnO-CuO nanocomposites were explored for MGSs such as flower-like (ethanol), nanorods (H₂S) (Kim, Jahan, et al., 2012) and three-dimensional inverse opal (3D IO) structures (acetone) (Xie et al., 2015). ZnO-CuO nanocomposites provide n-p type heterojunction that stems from a combination of ZnO (n-type) and CuO (p-type) where the fabrication of such heterojunction can lead to increased resistance as an output signal when compared to pure ZnO and CuO (Xie et al., 2015). 3D IO ZnO-CuO nanocomposite with well-ordered pores was evaluated for sensing acetone at LOD = 0.1 ppm in breath. The acetone concentration in the exhaled breath of healthy people is approximately 0.3 to 0.9 ppm and that in diabetic patients, type 1 and type 2, is 2.2 ppm and 1.7 ppm, respectively; therefore, the latter sensor can meet the requirement of the proper dynamic linear range and LOD for diabetic diagnosis (Table 2) (da Silva et al., 2016). The interaction between the metal oxide and gases occurs near the surface of metal oxide. However, porous structures not only have active sites near the surface but also have channels at the inner sites that give rise to the number of reaction sites and thereby the sensitivity (Kim, Choi, et al., 2016). 3D IO ZnO-Fe₃O₄ nanocomposite also indicated high sensitivity for the detection of acetone, while the overall analytical performance of MGS based on 3D IO ZnO-CuO nanocomposite is superior to 3D IO ZnO-Fe₃O₄ nanocomposite (Table 2) (Zhang et al., 2017). The role of ZnO morphologies in the detection of the target gas was studied, and as a result, 3D IO ZnO response towards acetone was 2.2 times more than ZnO nanoparticles due to the large surface-to-volume ratio of 3D IO morphology that boosted the sensitivity by providing more active sites. The high operating temperature in these two works limits their practical applications for breath analysis as per their high-energy consumption and difficult operation.

Importantly, high operating temperature reduces the discrimination capability of MGS in actual breath since voltaic organic compounds might be unstable and decomposed to other compounds.

Metal doping enhances the selectivity of gas sensors and amplifies the response towards the target gas (Kim, Ahn, et al., 2016). Additionally, metal doping leads to rapid response and recovery time. Ti doping on ZnO by flame spray reactor led to good isoprene sensing abilities. The preparation method for Ti-ZnO particles is illustrated in Figure 1A where Zn and Ti metal ions mixed before spray (Guntner et al., 2016). The incorporation of Ti⁴⁺ reduced the particle and crystal size of ZnO by which could further enhance the sensitivity. Isoprene gas is employed for monitoring the high level of cholesterol (Guntner et al., 2016). Treatment with atorvastatin led to the reduction in the exhaled isoprene level suggesting isoprene as a predicting biomarker for evaluating the efficiency of treatment in a rapid manner (Karl et al., 2001). Ce-doped ZnO amplified the response to acetone at room temperature (RT) owing to the generation of various cerium species (Ce²⁺, Ce³⁺ and Ce⁴⁺) that produced many oxygen vacancies for electron transportation with metal oxides and the target gas (Kulandaisamy et al., 2016). However, at RH equal to 54 humidity of breath is not mimicked. In addition to Ce, Pt and La doping on ZnO presented great sensitive materials for acetone detection, as discussed in the following.

The integration of Pt nanomaterials into a sensing platform has been widely reported owing to the high catalytic activity of these nanoparticles in the redox process that enhances sensing characteristics (Cho et al., 2017; Haghshenas et al., 2020). Notably, the methodology for the incorporation of nanomaterial into ZnO plays a significant role in ensuring its catalytic activity in the absence of agglomeration. To provide functional Pt, La and Cu nanoparticles for the modification of ZnO nanofibres, Cho et al. applied the protein template termed apoferritin followed by calcination as shown in Figure 1B (Cho et al., 2017). With the use of apoferritin, the repulsive forces between protein shells not only inhibited the aggregation of nanoparticles but also significantly improved the size distribution of Pt through the encapsulation in apoferritin nanocages. Pt-functionalized ZnO nanofibre implied the response ($R_{air}/R_{gas} = 13.07$) towards acetone compared with the response ($R_{air}/R_{gas} = 2.05$) of ZnO nanofibres. The catalytic activity of Cu-ZnO nanofibres resulted in ($R_{air}/R_{gas} = 6.04$) and that of La-ZnO nanofibres led to the responses ($R_{air}/R_{gas} = 10.6$) towards acetone. Similar gas sensors were reported somewhere else where WO₃ nanofibres were modified with Pt nanoparticles using apoferritin (Kim et al., 2017; Kim, Choi, et al., 2016).

Operational temperature plays a critical role in the sensing efficiency of MGS. The response of hierarchical ZnO gas sensor towards acetone, as a function of the operating temperature, was studied; the unique U-shape response attributed to the oxidizing and reducing behaviour of acetone at 25°C and 200°C, respectively (Singh et al., 2019). This study further highlights the challenges associated with MGS rely on high operational temperature regardless of the behaviour of exhaled breath compounds. It is of note that high operational temperature may change the selectivity of MGS (Nguyen

TABLE 2 ZnO, SnO₂ and In₂O₃-based gas sensors

Sensitive material	Target gas	Operational temperature	Detection range (ppm)	LOD (ppm)	RH%	Reference
3D inverse opal ZnO-CuO	Acetone	310°C	0.2–50	0.1	93	Xie et al. (2015)
Ti-ZnO	Isoprene	325°C	20–500	9.3	90	Guntner et al. (2016)
Ce-ZnO	Acetone ethanalamine	RT	1–100	1	54	Kulandaisamy et al. (2016)
		RT	1–500	-	54	
Pt-ZnO	Acetone	450°C	1–5	-	95	Cho et al. (2017)
Cu-ZnO	Acetone	450°C	1–5	-	95	
La-ZnO	NO	400°C	1–5	-	95	
ZnO hierarchical	Acetone	RT and 200°C	1–5	1	5	Chen et al. (2017)
3D inverse opal ZnO-Fe ₃ O ₄	Acetone	485°C	-	0.1	20	Zhang et al. (2017)
Ag nanowire-ZnO nanorods	NO	RT	0.01–0.1	0.01	10	Singh et al. (2019)
Nanospiral ZnO film	NO	150C	10–100	10	40	Luo et al. (2020)
Pt-SnO ₂ nanotubes	H ₂ S	300°C	0.1–0.6	0.1	95	Bulemo et al. (2017)
Pd-SnO ₂ nanowires	H ₂	150°C	10–100	-	-	Nguyen et al. (2017)
RGO-SnO ₂	Ethanol	300°C	43–100	-	98	Zito et al. (2017)
SnO ₂ nanoparticles	H ₂	450°C	100–500	1	80	Vasiliev et al. (2018)
PdAu-SnO ₂	Formaldehyde	110°C	-	45	94	Li et al. (2019)
	Acetone	250°C	-	30	94	
Au@WO ₃ SnO ₂ nanofibres	Acetone	150°C	0.2–10	-	90	Shao et al. (2019)
SnO ₂ /rGO/PANI	H ₂ S	RT	0.05–10	0.05	97	Zhang et al. (2019)
Pt@In ₂ O ₃ core-shell nanowires	Acetone	320°C	-	0.01	100	Liu et al. (2018)
Pt-In ₂ O ₃ mesoporous nanofibres	Acetone	180°C	0.01–50	0.01	85	Liu et al. (2019)
PA/Gr/nanoribbon/In ₂ O ₃	NH ₃	RT	0.65–1.69	0.65	-	Xu and Wu (2020)

Abbreviations: Gr, graphene; PANI, polyaniline; RGO, reduced graphene oxide; RT, room temperature.

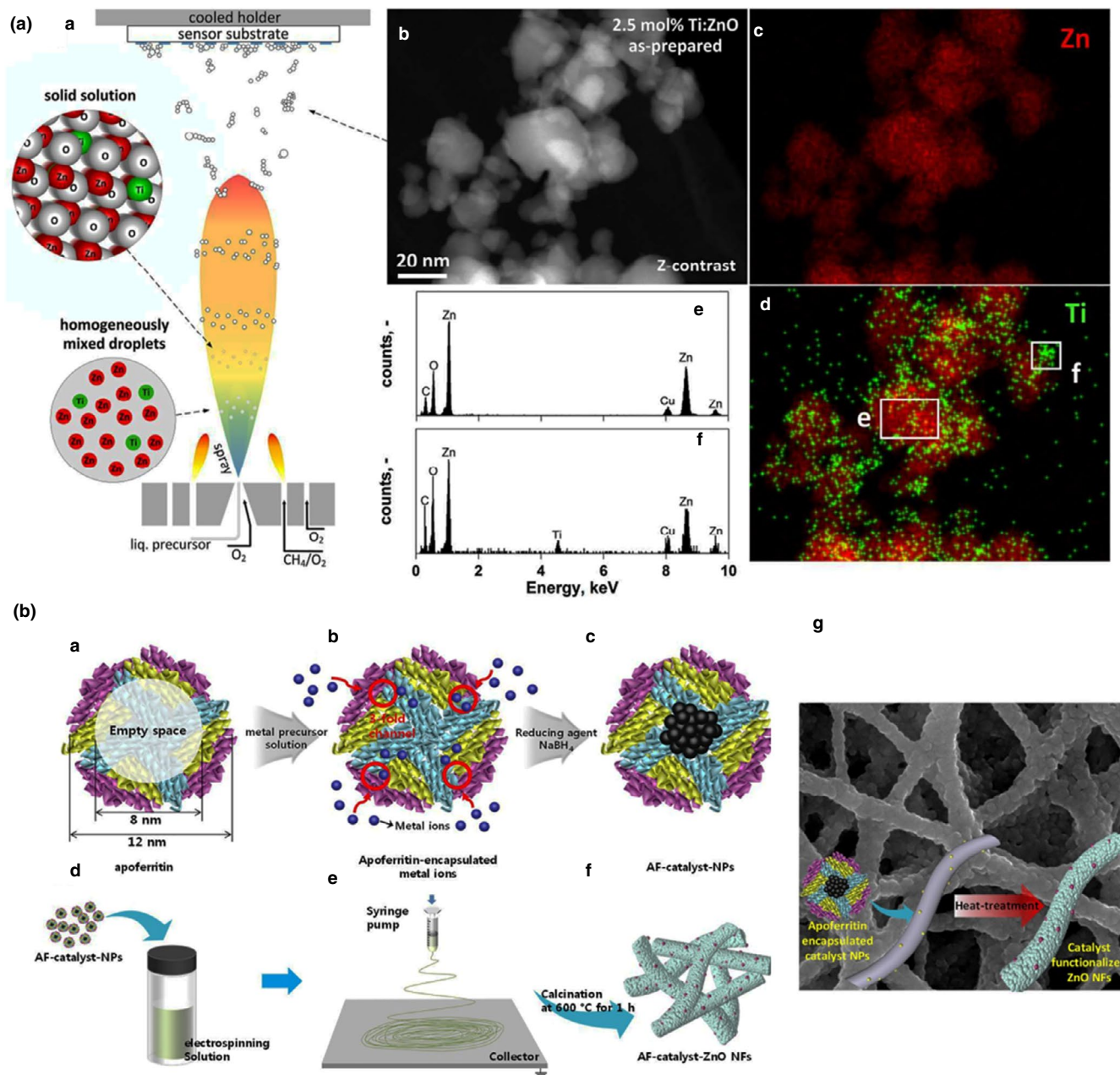


FIGURE 1 ZnO metal oxide preparation approach for gas sensors. A. (a) Schematic of the preparation process of Ti-doped ZnO by the flame spray in which the products were directly deposited on the sensing platform. (b) STEM morphology image of Ti-doped ZnO. Elemental mapping of Zn distribution (red) in (c) and Ti distribution (green) in (d). EDX (e, f) of the selected area in (d); reproduced from Guntner et al. (2016) with the permission from The Royal Society of Chemistry. B. Schematic of the preparation process of nanomaterials with a protein template named apoferritin. (g) The SEM image of Pt-ZnO nanofibres after calcination (Cho et al., 2017)

et al., 2017). Therefore, developing MGS that enabled to work at room temperature is desirable.

3.2 | SnO₂-based gas sensors

SnO₂ (n-type semiconductor) is one of the most explored metal oxides in MGS fields owing to its outstanding stability, wide bandgap and excellent electron mobility. SnO₂ with various morphologies, such as powder (Cirera et al., 1999), nanowire (Hwang et al., 2011;

Wang et al., 2008), nanotube (Bulemo et al., 2017), SnO₂-ZnO core-shell nanofibre (Choi et al., 2009) and SnO₂-ZnO core-shell nanospheres (Zhang, Zhou, et al., 2016), was studied in gas sensors. In an interesting study, the preparation of porous SnO₂ nanotubes was reported from SiO₂-SnO₂ composites after SiO₂ etching followed by the decoration of exteriors and interiors walls with Pt nanoparticles (Figure 2) (Bulemo et al., 2017). This sensing platform revealed a remarkable response ($R_{\text{air}}/R_{\text{gas}} = 89.3$) towards 1 ppm H₂S. Excellent surface area, nanosize crystals and the exceptional electrocatalytic property of Pt nanoparticles led to remarkable sensing performance.

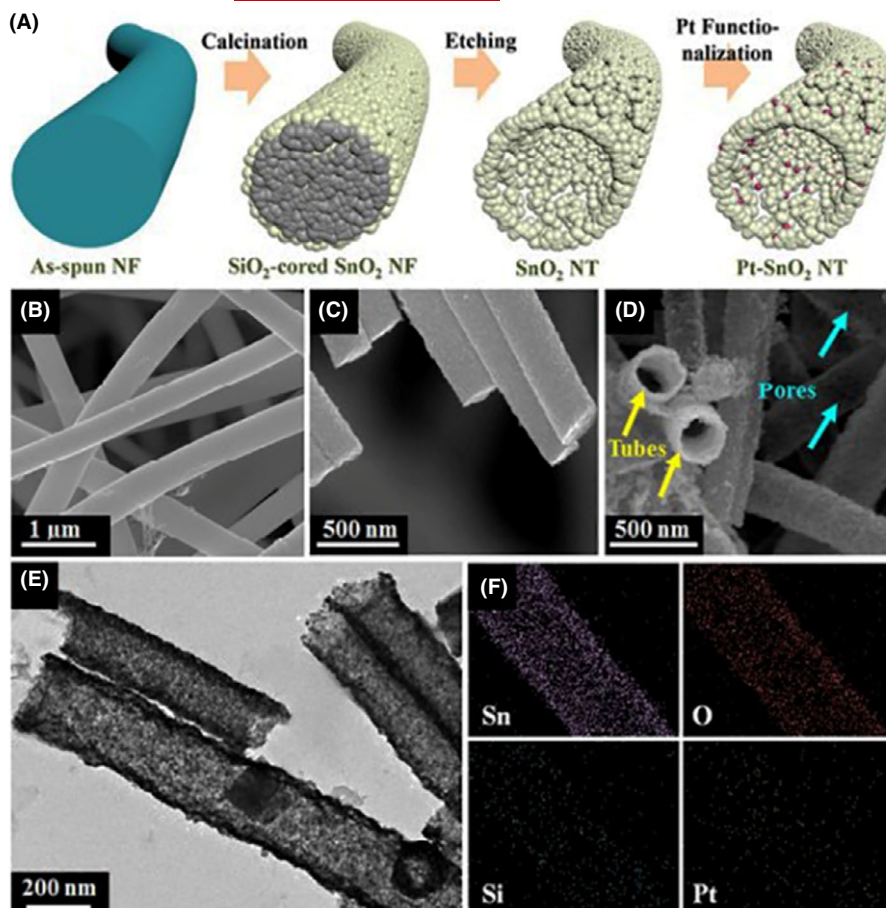


FIGURE 2 Gas sensor based on Pt-decorated SnO₂ nanotubes. (A) Schematic of the preparation process of Pt-decorated SnO₂ nanotubes. (B) Electrospinning nanofibres. (C) SiO₂-cored SnO₂ nanofibres. (D) SnO₂ nanotubes, (E) TEM image of Pt-SnO₂ nanotubes, EDS mapping of Pt-SnO₂ (F); reprinted with the permission from Bulemo et al. (2017), Copyright (2017) American Chemical Society

The high RH (95%) superior sensing performance of this gas sensor is attributed to residual SiO₂ that is responsible for humidity adsorption, while it did not contribute to H₂S sensing because of dielectric characterization.

SnO₂-based metal oxide sensors often need high operational temperature for gas sensing, and this increases the power consumption and shortens the lifetime of a sensor. To solve this issue, the Pd layer was deposited on SnO₂ nanowires prepared through on-chip growth approach. As a result, it lowered the operational temperature for the detection of H₂ to 150°C, while bare SnO₂ nanowires were comparably able to detect H₂ at a temperature of higher 350°C (Nguyen et al., 2017). Additionally, the selectivity of the gas sensor chip was evaluated in the presence of CO₂ and ethanol as interferences. Although the sensor did not indicate enough selectivity in ethanol, the response was remarkable for the detection of H₂ in the presence of CO₂. High operational temperature (150°C in this case) might be the reason for the low selectivity of this sensor as the behaviour of gases at high temperature is complex. Some images from this gas sensor chip are shown in Figure 3.

The low sensitivity of MGS particularly at high RH of the exhaled breath is one of the greatest challenges of gas sensors. This is due to the presence of superficial hydroxyl groups on metal oxides that conclude in undesirable reactions with false results. To reduce the number of hydroxyl groups on metal oxide surfaces, dry synthesis of

nanomaterials and high-temperature annealing is suggested (Vasiliev et al., 2018). In a study, a spark discharge approach was applied for the dry synthesis of SnO₂ to generate airborne SnO₂ nanoparticles, which are separated with air gap for the purpose of H₂ detection (Vasiliev et al., 2018). Additionally, surface saturation of metal oxide with hydroxyl groups could provide highly sensitive MGS at high RH since they do not adsorb more hydroxyl groups.

With a synergistic effect, the decoration of metal oxides with bimetallic nanoparticles is superior to their individuals for enhancing the sensitivity of MGS. Bimetallic nanoparticle decoration tailors the surface electronic structure of metal oxide and reduces the activation surface energy, and as a result, facilitates the electron transport for sensitive target detection. Generally, to ensure the high catalytic performance of bimetallic nanoparticles when integrated into MGS the size, morphology, dispersibility and also compatibility of bimetallic nanoparticles with metal oxide substrate should be taken into consideration (Kim et al., 2017). In a study, SnO₂ nanosheets with flower-like morphology decorated with PdAu bimetallic nanoparticles showed an excellent sensing platform for the detection of acetone at 250°C with features of reusability and reliability at high RH (Li et al., 2019). PdAu-SnO₂ had the sensitivity towards formaldehyde at the temperature of 110°C. This study highlighted the concern about the cross-sensitivity in an actual breath when the temperature is high.

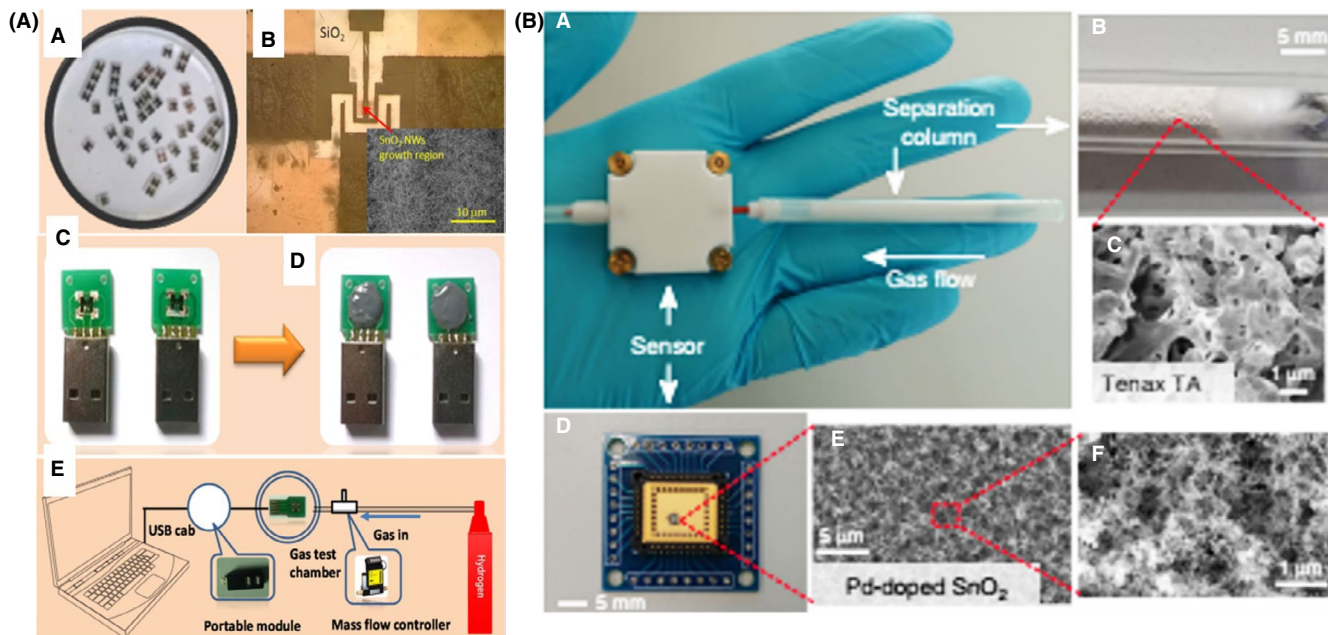


FIGURE 3 Metal oxide-based gas sensor. (a) Fabrication of the sensor chip on the glass substrate. (b) SEM images of SnO₂ nanowires as sensing material prepared through growing on a chip. (c, d) Sensor packaging. (e) Schematic of the setup of sensor chip (Nguyen et al., 2017)

The majority of current MGS suffered from low selectivity. Many researchers focus on the optimization of the experimental conditions to overcome this problem. However, developing MGS that relies on EBM separation with a filter and membrane holds a great promise for improving the selectivity of MGS, even in the cases that the materials do not have enough selectivity towards the target gas (Gregis et al., 2018).

Reduced graphene oxide, as a two-dimensional nanostructure, with excellent surface-to-volume ratio, low toxicity and outstanding electron mobility ($200,000 \text{ cm}^2 \text{ V}^{-1} \text{ s}^{-1}$), has been widely utilized for disease monitoring (Feng et al., 2017; Lee et al., 2018; Vajhadin et al., 2020; Zhang et al., 2018). In addition to graphene, other two-dimensional materials such as 2D-SnSe₂ and Ti₃C₂MXene have employed for producing flexible MGS owing to lightweight, outstanding flexibility and low cost (Sun et al., 2020; Tannarana et al., 2020). Recently, Lee et al. reviewed carbon-based materials such as graphene oxide as a sensing substrate for the detection of NO₂ gas (Lee et al., 2018). The nanocomposite of reduced graphene oxide and SnO₂ indicated the enhanced sensitivity for ethanol detection compared with hollow SnO₂ nanostructures in humid and dry conditions (Figure 4) (Zito et al., 2017).

The combination of reduced graphene oxide (p-type), polyaniline (p-type) and SnO₂ (n-type) served as a flexible sensing platform for the detection of very low concentration of H₂S (0.05 ppm) (Figure 5) (Zhang et al., 2019). Data processing for the recognition of H₂S through principal component analysis (PCA) was beneficial to improve the quality and reliability of their sensor. Generally, data analysis methods, including PCA, partial least squares (PLS), neural networks and Gaussian mixture models (GMMs), hold the potential to differentiate the target EBM among thousand EBM in exhaled breath (Rahman et al., 2020).

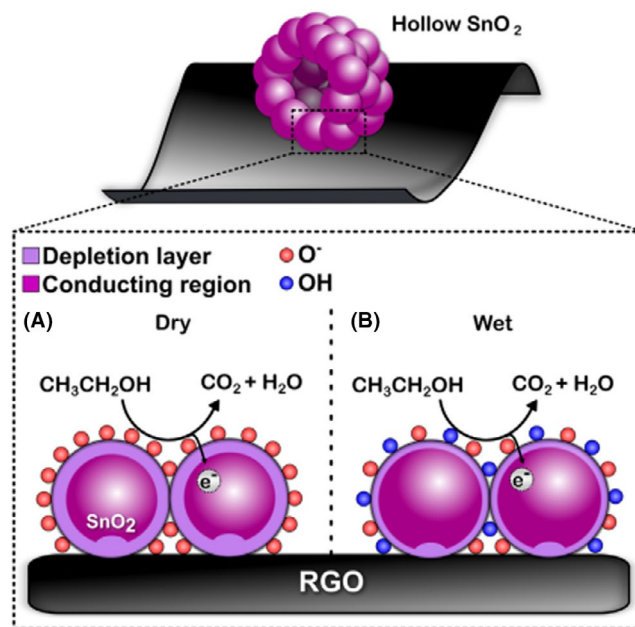


FIGURE 4 Schematic illustration of ethanol monitoring using reduced graphene oxide-SnO₂ nanocomposites substrate in dry and humid conditions (Zito et al., 2017). Electron transfers from SnO₂ to reduced graphene oxide that results in increasing depletion layer in SnO₂. In humid conditions, the formation of Sn-OH led to a reduction in the depletion layer of SnO₂ hollow nanospheres and thereby reduction in the resistance resulting in the decrease in ethanol responses

3.3 | In₂O₃-based gas sensors

In₂O₃ metal oxide has recently emerged as a promising metal oxide for MGS; however, its potential as a sensing material has been less

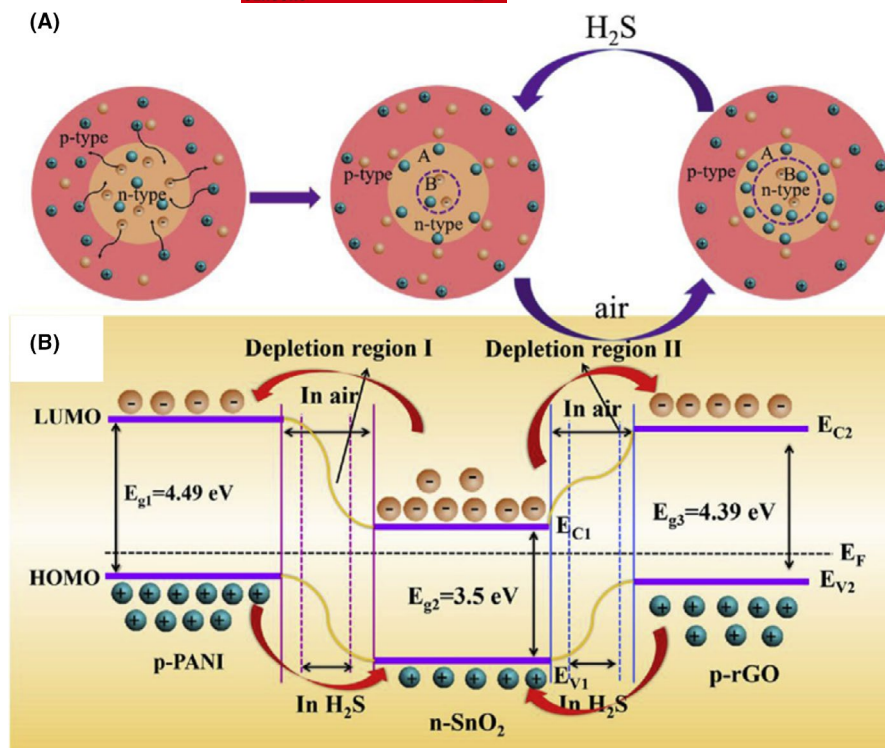


FIGURE 5 (A) Schematic illustration of the interaction between p-type and n-type materials to H_2S . (B) P-n heterojunction in the $\text{SnO}_2/\text{rGO}/\text{PANI}$ nanocomposite (Zhang et al., 2019). In the presence of the H_2S , the thickness of the electron depletion layers is decreased resulting in a decrease in the sensor resistance

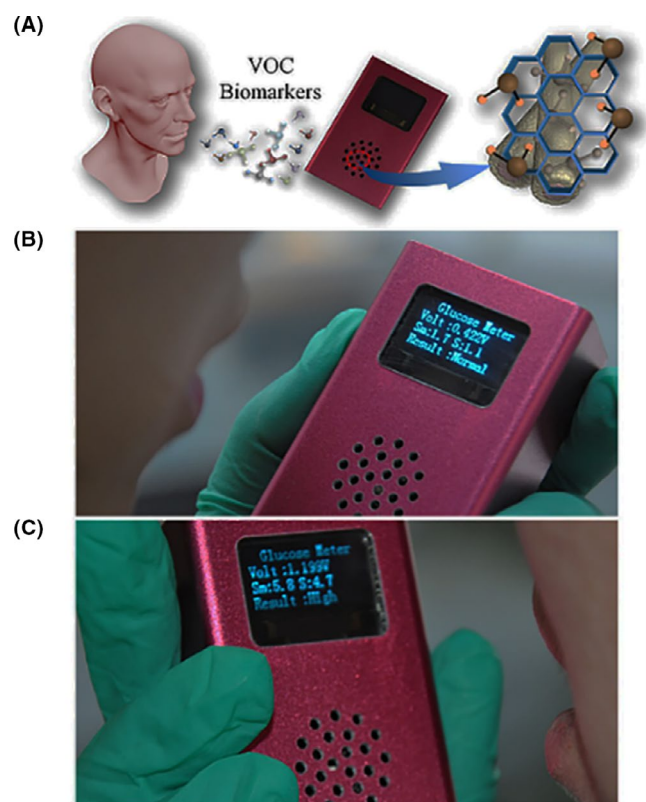


FIGURE 6 A portable gas sensor based on $\text{Pt@In}_2\text{O}_3$ nanowire for real-time acetone monitoring (Liu et al., 2018). (A) Schematic of the gas sensor performance. The sensor response for measuring acetone in exhaled breath of healthy (B) and diabetic (C) volunteers

exploited compared with ZnO and SnO_2 . In an interesting study, a portable gas sensor was fabricated using $\text{Pt@In}_2\text{O}_3$ core-shell nanowires for real-time acetone measurement in exhaled breath (Figure 6) (Liu et al., 2018). $\text{Pt@In}_2\text{O}_3$ core-shell structures, prepared by the co-electrospinning approach, lowered the measured LOD to 0.01 ppm at the operational temperature 320°C . Additionally, the parallel moisture resistance layer (mesoporous silica molecular sieve) that covered the sensing materials led to the functionality of the gas sensor at $\text{RH} \sim 100$. Liu et al also reported another gas sensor for the detection of acetone by Pt-decorated In_2O_3 mesoporous structures at a lower operational temperature (180°C) with very rapid response and recovery time of 6 s and 9 s, respectively (W. Liu et al., 2019). Besides, the sensor indicated high stability for 150 days that can be attributed to SnO_2 and the doping effect.

4 | CONCLUSIONS AND PERSPECTIVES

Rapid advancement in MGS leads to non-invasive and rapid monitoring of diseases on the basis of EBM. In this study, we reviewed the latest advances in metal oxide-based gas sensors for the detection of EBM with a focus on ZnO , SnO_2 and In_2O_3 owing to their unique sensing properties, satisfying stability and high compatibility for embedding into miniaturized chips. Despite progress in MGS, it is not profitable to use the majority of MGSs out of laboratories on a large scale. In fact, they are in their infancy and much more efforts needed to produce portable MGS to accurately characterize EBM in the actual exhaled breath. Generally, the bottlenecks of current MGS are as follows: (i) poor selectivity due to the difficulty

of recognition of EBM among various chemically similar molecules; (ii) unreliable responses at high RH (~100%) that mimics the amount of moisture in the exhaled breath; and (iii) high operational temperature that restrains the practical application of MGS for breath analysis. Coupling MGS with separation columns or membranes would significantly reduce the concern about the selectivity of the current MGS. In addition, statistically processing MGS responses elevates the selective detection by MGS. Utilizing new humidity-resistance composites in MGS leads to functional MGS in the humidity of breath.

ACKNOWLEDGEMENTS

The authors thank Yazd University for the funding support.

CONFLICT OF INTEREST

The authors declare that they have no known competing financial interests or personal relationships that could have appeared to influence the work reported in this paper.

REFERENCES

- Alkhoury, N., Singh, T., Alsabbagh, E., Guirguis, J., Chami, T., Hanouneh, I., Grove, D., Lopez, R., & Dweik, R. (2015). Isoprene in the exhaled breath is a novel biomarker for advanced fibrosis in patients with chronic liver disease: A pilot study. *Clinical and Translational Gastroenterology*, 6, e112. <https://doi.org/10.1038/ctg.2015.40>
- Amiri, V., Roshan, H., Mirzaei, A., Neri, G., & Ayesh, A. I. (2020). Nanostructured metal oxide-based acetone gas sensors. A review. *Sensors (Basel)*, 20(11), 3096. <https://doi.org/10.3390/s20113096>
- Barnes, P. J., Chowdhury, B., Kharitonov, S. A., Magnussen, H., Page, C. P., Postma, D., & Saetta, M. (2006). Pulmonary biomarkers in chronic obstructive pulmonary disease. *American Journal of Respiratory and Critical Care Medicine*, 174(1), 6–14. <https://doi.org/10.1164/rccm.200510-1659PP>
- Birrell, M., McCluskie, K., Hardaker, E., Knowles, R., & Belvisi, M. (2006). Utility of exhaled nitric oxide as a noninvasive biomarker of lung inflammation in a disease model. *European Respiratory Journal*, 28(6), 1236–1244.
- Brindicci, C., Ito, K., Resta, O., Pride, N. B., Barnes, P. J., & Kharitonov, S. A. (2005). Exhaled nitric oxide from lung periphery is increased in COPD. *European Respiratory Journal*, 26(1), 52–59. <https://doi.org/10.1183/09031936.04.00125304>
- Brinkman, P., Ahmed, W. M., Gómez, C., Knobel, H. H., Weda, H., Vink, T. J., Nijssen, T. M., Wheelock, C. E., Dahlen, S.-E., Montuschi, P., Knowles, R. G., Vijverberg, S. J., Maitland-van der Zee, A. H., Sterk, P. J., & Fowler, S. J. (2020). Exhaled volatile organic compounds as markers for medication use in asthma. *European Respiratory Journal*, 55(2), 1900544. <https://doi.org/10.1183/13993003.00544-2019>
- Bulemo, P. M., Cho, H. J., Kim, N. H., & Kim, I. D. (2017). Mesoporous SnO₂ nanotubes via electrospinning-etching route: highly sensitive and selective detection of H₂S molecule. *ACS Applied Materials & Interfaces*, 9(31), 26304–26313. <https://doi.org/10.1021/acsami.7b05241>
- Cazzola, M., & Novelli, G. (2010). Biomarkers in COPD. *Pulmonary Pharmacology & Therapeutics*, 23(6), 493–500. <https://doi.org/10.1016/j.pupt.2010.05.001>
- Chang, J.-E., Lee, D.-S., Ban, S.-W., Oh, J., Jung, M. Y., Kim, S.-H., Park, S. J., Persaud, K., & Jheon, S. (2018). Analysis of volatile organic compounds in exhaled breath for lung cancer diagnosis using a sensor system. *Sensors and Actuators B: Chemical*, 255, 800–807. <https://doi.org/10.1016/j.snb.2017.08.057>
- Chen, J., Pan, X., Boussaid, F., McKinley, A., Fan, Z., & Bermak, A. (2017). Breath level acetone discrimination through temperature modulation of a hierarchical ZnO gas sensor. *IEEE Sensors Letters*, 1(5), 1–4. <https://doi.org/10.1109/lsens.2017.2740222>
- Cho, H.-J., Kim, S.-J., Choi, S.-J., Jang, J.-S., & Kim, I.-D. (2017). Facile synthetic method of catalyst-loaded ZnO nanofibers composite sensor arrays using bio-inspired protein cages for pattern recognition of exhaled breath. *Sensors and Actuators B: Chemical*, 243, 166–175. <https://doi.org/10.1016/j.snb.2016.11.137>
- Choi, S.-W., Park, J. Y., & Kim, S. S. (2009). Synthesis of SnO₂-ZnO core-shell nanofibers via a novel two-step process and their gas sensing properties. *Nanotechnology*, 20(46), 465603.
- Chung, K. F. (2014). Hydrogen sulfide as a potential biomarker of asthma. *Expert Review of Respiratory Medicine*, 8(1), 5–13.
- Cirera, A., Dieguez, A., Diaz, R., Cornet, A., & Morante, J. (1999). New method to obtain stable small-sized SnO₂ powders for gas sensors. *Sensors and Actuators B: Chemical*, 58(1–3), 360–364.
- Crofford, O. B., Mallard, R. E., Winton, R. E., Rogers, N. L., Jackson, J. C., & Keller, U. (1977). Acetone in breath and blood. *Transactions of the American Clinical and Climatological Association*, 88, 128–139.
- da Silva, L. F., Catto, A. C., Avansi, W., Cavalcante, L. S., Mastelaro, V. R., Andrés, J., Aguir, K., & Longo, E. (2016). Acetone gas sensor based on α -Ag₂WO₄ nanorods obtained via a microwave-assisted hydrothermal route. *Journal of Alloys and Compounds*, 683, 186–190. <https://doi.org/10.1016/j.jallcom.2016.05.078>
- Das, S., & Pal, M. (2020). Review—Non-invasive monitoring of human health by exhaled breath analysis: A comprehensive review. *Journal of the Electrochemical Society*, 167(3), 37562. <https://doi.org/10.1149/1945-7111/ab67a6>
- Feng, Q., Li, X., & Wang, J. (2017). Percolation effect of reduced graphene oxide (rGO) on ammonia sensing of rGO-SnO₂ composite based sensor. *Sensors and Actuators B: Chemical*, 243, 1115–1126. <https://doi.org/10.1016/j.snb.2016.12.075>
- Ferrus, L., Guenard, H., Vardon, G., & Varene, P. (1980). Respiratory water loss. *Respiration Physiology*, 39(3), 367–381. [https://doi.org/10.1016/0034-5687\(80\)90067-5](https://doi.org/10.1016/0034-5687(80)90067-5)
- Glockler, J., Jaeschke, C., Kocaoz, Y., Kokoric, V., Tutuncu, E., Mitrovics, J., & Mizaiokoff, B. (2020). iHWG-MOX: A hybrid breath analysis system via the combination of substrate-integrated hollow waveguide infrared spectroscopy with metal oxide gas sensors. *ACS Sensors*, 5(4), 1033–1039. <https://doi.org/10.1021/acssensors.9b02554>
- Gregis, G., Sanchez, J.-B., Bezverkhyy, I., Guy, W., Berger, F., Fierro, V., Bellat, J.-P., & Celzard, A. (2018). Detection and quantification of lung cancer biomarkers by a micro-analytical device using a single metal oxide-based gas sensor. *Sensors and Actuators B: Chemical*, 255, 391–400. <https://doi.org/10.1016/j.snb.2017.08.056>
- Guntner, A. T., Abegg, S., Königstein, K., Gerber, P. A., Schmidt-Trucksass, A., & Pratsinis, S. E. (2019). Breath sensors for health monitoring. *ACS Sensors*, 4(2), 268–280. <https://doi.org/10.1021/acssensors.8b00937>
- Guntner, A. T., Pineau, N. J., Chie, D., Krumeich, F., & Pratsinis, S. E. (2016). Selective sensing of isoprene by Ti-doped ZnO for breath diagnostics. *Journal of Materials Chemistry B*, 4(32), 5358–5366. <https://doi.org/10.1039/c6tb01335j>
- Haghshenas, M., Mazloum-Ardakani, M., Alizadeh, Z., Vajhadin, F., & Naeimi, H. (2020). A sensing platform using Ag/Pt core-shell nanostructures supported on multiwalled carbon nanotubes to detect hydroxyurea. *Electroanalysis*, 32, 1–10. <https://doi.org/10.1002/elan.202060020>
- Hanh, N. H., Van Duy, L., Hung, C. M., Van Duy, N., Heo, Y.-W., Van Hieu, N., & Hoa, N. D. (2020). VOC gas sensor based on hollow cubic assembled nanocrystal Zn₂SnO₄ for breath analysis. *Sensors and Actuators A: Physical*, 302, 111834. <https://doi.org/10.1016/j.sna.2020.111834>
- Ho, C.-H., Chan, C.-H., Tien, L.-C., & Huang, Y.-S. (2011). Direct optical observation of band-edge excitons, band gap, and Fermi level in

- degenerate semiconducting oxide nanowires In₂O₃. *The Journal of Physical Chemistry C*, 115(50), 25088–25096.
- Hwang, I.-S., Choi, J.-K., Woo, H.-S., Kim, S.-J., Jung, S.-Y., Seong, T.-Y., & Lee, J.-H. (2011). Facile control of C₂H₅OH sensing characteristics by decorating discrete Ag nanoclusters on SnO₂ nanowire networks. *ACS Applied Materials & Interfaces*, 3(8), 3140–3145.
- Kabir, E., Raza, N., Kumar, V., Singh, J., Tsang, Y. F., Lim, D. K., Szulejko, J. E., & Kim, K.-H. (2019). Recent advances in nanomaterial-based human breath analytical technology for clinical diagnosis and the way forward. *Chemistry*, 5(12), 3020–3057. <https://doi.org/10.1016/j.chempr.2019.08.004>
- Karl, T., Prazeller, P., Mayr, D., Jordan, A., Rieder, J., Fall, R., & Lindinger, W. (2001). Human breath isoprene and its relation to blood cholesterol levels: new measurements and modeling. *Journal of Applied Physiology*, 91(2), 762–770. <https://doi.org/10.1152/jappl.2001.91.2.762>
- Kharitonov, S., & Barnes, P. (1996). Nitric oxide in exhaled air is a new marker of airway inflammation. *Monaldi Archives for Chest Disease. Archivio Monaldi per Le Malattie Del Torace*, 51(6), 533.
- Kharitonov, S. A., & Barnes, P. J. (2002). Biomarkers of some pulmonary diseases in exhaled breath. *Biomarkers*, 7(1), 1–32. <https://doi.org/10.1080/13547500110104233>
- Kim, B. Y., Ahn, J. H., Yoon, J. W., Lee, C. S., Kang, Y. C., Abdel-Hady, F., & Lee, J. H. (2016). Highly selective xylene sensor based on NiO/NiMoO₄ nanocomposite hierarchical spheres for indoor air monitoring. *ACS Applied Materials & Interfaces*, 8(50), 34603–34611. <https://doi.org/10.1021/acsmi.6b13930>
- Kim, J., Kim, W., & Yong, K. (2012). CuO/ZnO Heterostructured Nanorods: Photochemical synthesis and the mechanism of H₂S gas sensing. *The Journal of Physical Chemistry C*, 116(29), 15682–15691. <https://doi.org/10.1021/jp302129j>
- Kim, K. H., Jahan, S. A., & Kabir, E. (2012). A review of breath analysis for diagnosis of human health. *TrAC Trends in Analytical Chemistry*, 33, 1–8. <https://doi.org/10.1016/j.trac.2011.09.013>
- Kim, S. J., Choi, S. J., Jang, J. S., Cho, H. J., Koo, W. T., Tuller, H. L., & Kim, I. D. (2017). Exceptional high-performance of Pt-based bimetallic catalysts for exclusive detection of exhaled biomarkers. *Advanced Materials*, 29(36), 1700737. <https://doi.org/10.1002/adma.201707037>
- Kim, S. J., Choi, S. J., Jang, J. S., Kim, N. H., Hakim, M., Tuller, H. L., & Kim, I. D. (2016). Mesoporous WO₃ nanofibers with protein-templated nanoscale catalysts for detection of trace biomarkers in exhaled breath. *ACS Nano*, 10(6), 5891–5899. <https://doi.org/10.1021/acsnano.6b01196>
- Kulandaisamy, A. J., Elavalagan, V., Shankar, P., Mani, G. K., Babu, K. J., & Rayappan, J. B. B. (2016). Nanostructured Cerium-doped ZnO thin film – A breath sensor. *Ceramics International*, 42(16), 18289–18295. <https://doi.org/10.1016/j.ceramint.2016.08.156>
- Lee, S. W., Lee, W., Hong, Y., Lee, G., & Yoon, D. S. (2018). Recent advances in carbon material-based NO₂ gas sensors. *Sensors and Actuators B: Chemical*, 255, 1788–1804. <https://doi.org/10.1016/j.snb.2017.08.203>
- Li, G., Cheng, Z., Xiang, Q., Yan, L., Wang, X., & Xu, J. (2019). Bimetal PdAu decorated SnO₂ nanosheets based gas sensor with temperature-dependent dual selectivity for detecting formaldehyde and acetone. *Sensors and Actuators B: Chemical*, 283, 590–601. <https://doi.org/10.1016/j.snb.2018.09.117>
- Liu, L., Fei, T., Guan, X., Lin, X., Zhao, H., & Zhang, T. (2020). Room temperature ammonia gas sensor based on ionic conductive biomass hydrogels. *Sensors and Actuators B: Chemical*, 320, 128318. <https://doi.org/10.1016/j.snb.2020.128318>
- Liu, W., Xie, Y., Chen, T., Lu, Q., Ur Rehman, S., & Zhu, L. (2019). Rationally designed mesoporous In₂O₃ nanofibers functionalized Pt catalysts for high-performance acetone gas sensors. *Sensors and Actuators B: Chemical*, 298, 126871. <https://doi.org/10.1016/j.snb.2019.126871>
- Liu, W., Xu, L., Sheng, K., Zhou, X., Dong, B., Lu, G., & Song, H. (2018). A highly sensitive and moisture-resistant gas sensor for diabetes diagnosis with Pt@In₂O₃ nanowires and a molecular sieve for protection. *NPG Asia Materials*, 10(4), 293–308. <https://doi.org/10.1038/s41427-018-0029-2>
- Lu, Z., Huang, W., Wang, L., Xu, N., Ding, Q., & Cao, C. (2018). Exhaled nitric oxide in patients with chronic obstructive pulmonary disease: a systematic review and meta-analysis. *International Journal of Chronic Obstructive Pulmonary Disease*, 13, 2695–2705. <https://doi.org/10.2147/COPD.S165780>
- Luo, P., Xie, M., Luo, J., Kan, H., & Wei, Q. (2020). Nitric oxide sensors using nanospiral ZnO thin film deposited by GLAD for application to exhaled human breath. *RSC Advances*, 10(25), 14877–14884. <https://doi.org/10.1039/d0ra00488j>
- McCluskie, K., Birrell, M. A., Wong, S., & Belvisi, M. G. (2004). Nitric oxide as a noninvasive biomarker of lipopolysaccharide-induced airway inflammation: possible role in lung neutrophilia. *Journal of Pharmacology and Experimental Therapeutics*, 311(2), 625–633.
- Moseley, P. T. (2017). Progress in the development of semiconducting metal oxide gas sensors: a review. *Measurement Science and Technology*, 28(8), 82001. <https://doi.org/10.1088/1361-6501/aa7443>
- Nguyen, K., Hung, C. M., Ngoc, T. M., Thanh Le, D. T., Nguyen, D. H., Nguyen Van, D., & Nguyen Van, H. (2017). Low-temperature prototype hydrogen sensors using Pd-decorated SnO₂ nanowires for exhaled breath applications. *Sensors and Actuators B: Chemical*, 253, 156–163. <https://doi.org/10.1016/j.snb.2017.06.141>
- Rahman, S., Alwadie, A. S., Irfan, M., Nawaz, R., Raza, M., Javed, E., & Awais, M. (2020). Wireless E-nose sensors to detect volatile organic gases through multivariate analysis. *Micromachines (Basel)*, 11(6), <https://doi.org/10.3390/mi11060597>
- Rudnicka, J., Kowalkowski, T., & Buszewski, B. (2019). Searching for selected VOCs in human breath samples as potential markers of lung cancer. *Lung Cancer*, 135, 123–129. <https://doi.org/10.1016/j.lungcan.2019.02.012>
- Ruzsanyi, V., & Peter Kalapos, M. (2017). Breath acetone as a potential marker in clinical practice. *Journal of Breath Research*, 11(2), 24002. <https://doi.org/10.1088/1752-7163/aa66d3>
- Salerno-Kennedy, R., & Cashman, K. D. (2005). Potential applications of breath isoprene as a biomarker in modern medicine: a concise overview. *Wiener Klinische Wochenschrift*, 117(5–6), 180–186. <https://doi.org/10.1007/s00508-005-0336-9>
- Shao, S., Chen, X., Chen, Y., Lai, M., & Che, L. (2019). Ultrasensitive and highly selective detection of acetone based on Au@WO₃-SnO₂ corrugated nanofibers. *Applied Surface Science*, 473, 902–911. <https://doi.org/10.1016/j.apsusc.2018.12.208>
- Singh, P., Hu, L. L., Zan, H. W., & Tseng, T. Y. (2019). Highly sensitive nitric oxide gas sensor based on ZnO-nanorods vertical resistor operated at room temperature. *Nanotechnology*, 30(9), 95501. <https://doi.org/10.1088/1361-6528/aaf7cb>
- Sun, S., Wang, M., Chang, X., Jiang, Y., Zhang, D., Wang, D., Zhang, Y., & Lei, Y. (2020). W₁₈O₄₉/Ti₃C₂T_x Mxene nanocomposites for highly sensitive acetone gas sensor with low detection limit. *Sensors and Actuators B: Chemical*, 304, 127274. <https://doi.org/10.1016/j.snb.2019.127274>
- Tai, H., Wang, S., Duan, Z., & Jiang, Y. (2020). Evolution of breath analysis based on humidity and gas sensors: Potential and challenges. *Sensors and Actuators B: Chemical*, 318, <https://doi.org/10.1016/j.snb.2020.128104>
- Tannarana, M., Solanki, G. K., Bhakhar, S. A., Patel, K. D., Pathak, V. M., & Pataniya, P. M. (2020). 2D-SnSe₂ Nanosheet functionalized Piezo-resistive flexible sensor for pressure and human breath monitoring. *ACS Sustainable Chemistry & Engineering*, 8(20), 7741–7749. <https://doi.org/10.1021/acssuschemeng.0c01827>
- Vajhadin, F., Ahadian, S., Travas-Sejdic, J., Lee, J., Mazloum-Ardakani, M., Salvador, J., Aninwene, G. E., Bandaru, P., Sun, W., &

- Khademhossieni, A. (2020). Electrochemical cytosensors for detection of breast cancer cells. *Biosensors and Bioelectronics*, 151, 111984. <https://doi.org/10.1016/j.bios.2019.111984>
- Vasiliev, A., Varfolomeev, A., Volkov, I., Simonenko, N., Arsenov, P., Vlasov, I., Ivanov, V., Pisyakov, A., Lagutin, A., Jahatspanian, I., & Maeder, T. (2018). Reducing humidity response of gas sensors for medical applications: Use of spark discharge synthesis of metal oxide nanoparticles. *Sensors (Basel)*, 18(8), 2600. <https://doi.org/10.3390/s18082600>
- Wang, B., Zhu, L., Yang, Y., Xu, N., & Yang, G. (2008). Fabrication of a SnO₂ nanowire gas sensor and sensor performance for hydrogen. *The Journal of Physical Chemistry C*, 112(17), 6643–6647.
- Wang, C., & Sahay, P. (2009). Breath analysis using laser spectroscopic techniques: breath biomarkers, spectral fingerprints, and detection limits. *Sensors (Basel)*, 9(10), 8230–8262. <https://doi.org/10.3390/s91008230>
- Wehinger, A., Schmid, A., Mechtcheriakov, S., Ledochowski, M., Grabmer, C., Gastl, G. A., & Amann, A. (2007). Lung cancer detection by proton transfer reaction mass-spectrometric analysis of human breath gas. *International Journal of Mass Spectrometry*, 265(1), 49–59. <https://doi.org/10.1016/j.ijms.2007.05.012>
- Wei, A., Pan, L., & Huang, W. (2011). Recent progress in the ZnO nanostructure-based sensors. *Materials Science and Engineering: B*, 176(18), 1409–1421. <https://doi.org/10.1016/j.mseb.2011.09.005>
- Xie, Y., Xing, R., Li, Q., Xu, L., & Song, H. (2015). Three-dimensional ordered ZnO–CuO inverse opals toward low concentration acetone detection for exhaled breath sensing. *Sensors and Actuators B: Chemical*, 211, 255–262. <https://doi.org/10.1016/j.snb.2015.01.086>
- Xu, L.-H., & Wu, T.-M. (2020). Synthesis of highly sensitive ammonia gas sensor of polyaniline/graphene nanoribbon/indium oxide composite at room temperature. *Journal of Materials Science: Materials in Electronics*, 31(9), 7276–7283. <https://doi.org/10.1007/s10854-020-03299-6>
- Zhang, D., Wu, Z., & Zong, X. (2019). Flexible and highly sensitive H₂S gas sensor based on in-situ polymerized SnO₂/rGO/PANI ternary nanocomposite with application in halitosis diagnosis. *Sensors and Actuators B: Chemical*, 289, 32–41. <https://doi.org/10.1016/j.snb.2019.03.055>
- Zhang, J., Liu, X., Neri, G., & Pinna, N. (2016). Nanostructured materials for room-temperature gas sensors. *Advanced Materials*, 28(5), 795–831. <https://doi.org/10.1002/adma.201503825>
- Zhang, J., Lu, H., Yan, C., Yang, Z., Zhu, G., Gao, J., Yin, F., & Wang, C. (2018). Fabrication of conductive graphene oxide-WO₃ composite nanofibers by electrospinning and their enhanced acetone gas sensing properties. *Sensors and Actuators B: Chemical*, 264, 128–138. <https://doi.org/10.1016/j.snb.2018.02.026>
- Zhang, J., Wang, X., Chen, Y., & Yao, W. (2015). Exhaled hydrogen sulfide predicts airway inflammation phenotype in COPD. *Respiratory Care*, 60(2), 251–258. <https://doi.org/10.4187/respcare.03519>
- Zhang, L., Dong, B., Xu, L., Zhang, X., Chen, J., Sun, X., Xu, H., Zhang, T., Bai, X., Zhang, S., & Song, H. (2017). Three-dimensional ordered ZnO–Fe₃O₄ inverse opal gas sensor toward trace concentration acetone detection. *Sensors and Actuators B: Chemical*, 252, 367–374. <https://doi.org/10.1016/j.snb.2017.05.167>
- Zhang, R., Zhou, T., Wang, L., Lou, Z., Deng, J., & Zhang, T. (2016). The synthesis and fast ethanol sensing properties of core-shell SnO₂@ZnO composite nanospheres using carbon spheres as templates. *New Journal of Chemistry*, 40(8), 6796–6802. <https://doi.org/10.1039/c6nj00365f>
- Zito, C. A., Perfecto, T. M., & Volanti, D. P. (2017). Impact of reduced graphene oxide on the ethanol sensing performance of hollow SnO₂ nanoparticles under humid atmosphere. *Sensors and Actuators B: Chemical*, 244, 466–474. <https://doi.org/10.1016/j.snb.2017.01.015>

How to cite this article: Vajhadin F, Mazloun-Ardakani M, Amini A. Metal oxide-based gas sensors for the detection of exhaled breath markers. *Med Devices Sens*. 2021;4:e10161. <https://doi.org/10.1002/mds3.10161>